

Article

Dynamic Power Flow Cascading Failure Analysis of Wind Power Integration with Complex Network Theory

Yushu Sun ¹ , Xisheng Tang ^{1,*}, Guowei Zhang ¹, Fufeng Miao ² and Ping Wang ³

¹ Institute of Electrical Engineering, Chinese Academy of Sciences, Haidian District, Beijing 100190, China; yushusun@mail.iee.ac.cn (Y.S.); zhangguowei@mail.iee.ac.cn (G.Z.)

² State Grid Henan Power Company Economic and Technological Research Institute, Zhengzhou 450052, China; miaoff@vip.126.com

³ Jiangsu Province Electrochemical Energy Storage Technology Key Laboratory, Taizhou 225500, China; wangping@shuangdeng.com.cn

* Correspondence: tang@mail.iee.ac.cn; Tel.: +86-10-82547108; Fax: +86-10-82547103

Received: 30 October 2017; Accepted: 6 December 2017; Published: 29 December 2017

Abstract: The impact of the rapid development of large-scale centralized wind power farms on the power system is drawing more and more attention. Some topics about grid-connected wind power are discussed from the view of complex network theory in this paper. Firstly, a complex network cascading failure model is established, combined with dynamic AC power flow (DACPF). Then, the IEEE 30 bus system is used to analyze its validity using the simulations of nodes removal, wind power integration, as well as the change of current and voltage boundaries. Furthermore, the influences of wind power before and after smoothing are investigated. Also, different wind power coupling locations are studied. Finally, some significant conclusions are obtained to provide references for large-scale wind power integration.

Keywords: wind power; complex network theory; cascading failure; dynamic AC power flow

1. Introduction

With the rapid development of the larger-scale interconnected power systems, the complexity of sizes and operations in power systems is increasing. This means that the stability, security and reliability of power system are facing an enormous challenge. Large blackouts have attracted more and more attention due to power systems suffering from declining stability, and even cascading failure events. The 2003 “8·14” blackout in North America, a load loss up to 61.8 GW, led to a huge economic loss of 30 billion dollars [1]. In the same year, the “8·28” blackout in London brought about a load loss of 724 MW and resulted in 500,000 passengers being trapped in the subway [2]. These large blackouts are triggered by the successive malfunction of plenty of elements, that is, cascading failure, always induced by an initial disturbance or event, for example, component failure, ground fault, protection malfunctioning, or a hostile environment.

Recently, large-scale and long-distance grid-connected wind power have brought a more prominent impact on the stable operation of power system owing to its intermittent and randomness. The probability of cascading failure is then increased. As we know, the power system is a typical complex network, which has plenty of nodes and lines, as well as complicated topology structure and operating characteristics. Therefore, cascading failure in grid-connected wind power system is analyzed based on complex network theory in this paper.

So far, complex network theory has been widely applied in power system stability analysis. Chowdhury et al. [3] use topological indices to analyze power system vulnerability with renewable

energy sources. Wang et al. [4] present complex network theory to identify the vulnerable lines of power system with a vulnerability index. Luo et al. [5] can identify transmission sections from three levels of transmission lines, key transmission links and partition sections automatically. Chu et al. [6] illustrate how complex network theory can be applied to modern smart grids in structural vulnerability assessment, cascading blackouts, network reconfigurations, and so on. Correa et al. [7] obtain a similar conclusion from the graph theory on electric network vulnerability by comparisons of physical power flow models and scale-free graph statistic indexes. Fan et al. [8] propose a cascading failure model based on complex network theory by combining the node overload failures and hidden failures of transmission lines in blackouts together. The simulation results are very useful for cascading failure propagation mechanism analysis and the protection strategy development against cascading failures in power grids.

A lot of research on cascading failures in power system has been done, and the most important relates to how to define the load in the established model. Yin et al. [9] define a function of node degree k_j , $F_j = k_j^\beta$, $j = 1, 2, \dots, N$, as initial load of each node j in the power grid. Here, the cascading failure of complex power networks is analyzed with the local preferential redistribution rule of the load of failure node. Zhang et al. [10] adopt $L_i = k_i (\sum_{m \in \Gamma_i} k_m)$ as an initial load of node i , where k_i is the degree of node i and Γ_i denotes the neighborhood of node i . Liu et al. [11] use $L_j = k_j (\sum_{m \in \Gamma_j} k_m)^\alpha$ as the load of a node j , where α is a tunable parameter. Zhang et al. [12] establish a similar model with complex network theory, where the initial load of node i is described as $L_i = \alpha k_i + (1 - \alpha) \sum_{j \in \Gamma_i} k_j$. Wang et al. [13] apply a cascading model using a local load redistribution rule. The initial load of edge ij is $L_i = (k_i k_j)^\alpha$, where k_i and k_j are the degrees of the nodes connected by the edge. Wang et al. [14] use $L_{ij} = \left[(k_i \sum_{a \in \Gamma_i} k_a) (k_j \sum_{b \in \Gamma_j} k_b) \right]^\alpha$ as the initial load of edge ij , and analyze the cascading phenomenon of uncorrelated scale-free networks with two different attack strategies on edges.

In power system, some nodes or edges have smaller degree, but play an important role in power transmission. Therefore, the concept of betweenness is introduced to reveal the propagation mechanism of network failure. Peng et al. [15] establish a network cascading failure model, where the number of shortest paths passing through a node (i.e., node betweenness) are defined as its load. Nicholson [16] uses betweenness as edge load to sort the critical edges for the implementation of preparedness options.

In the analysis of betweenness, power transmission between two nodes is supposed to pass the shortest path, which is far from Kirchhoff's law. Power transmission from a generator node to a load node will be undertaken by all possible lines. Bompard et al. [17] define an extended betweenness centrality considering the complex characteristics of power system. The local importance of the components in power system can also be measured. Bompard [18] and Yan [19] et al. propose a joint method of extended betweenness to define electric power load considering network structure and electrical characteristics. By using this power transfer distribution factor-based model (i.e., extended betweenness), the most critical lines and buses in an electrical power grid can be evaluated. Lin et al. [20] propose a self-healing transmission network reconfiguration algorithm based on the complex network theory to analyze the capacities of generators and the amounts of high priority loads, as well as the distribution and importance of each transmission line.

However, the extended or electrical betweenness identifies the critical nodes or lines from the perspective of topological structure without considering the operational states of power system. Yan et al. [21] discuss the validity of a typical DC power flow-based cascading failure simulator in cascading failure analysis using the critical moment. Qi et al. [22] use the probabilistic power flow combined with DC power flow model to analyze single line failure probability. Chen et al. [23] embed a DC power flow model with hidden failures into the traditional error and attack tolerance methodology to develop a new approach for power system vulnerability modeling and assessment.

DC power flow model is modeled with linear equations, so it does not accurately reflect the nonlinear characteristics of the power system. Dwivedi et al. [24] explore a new centrality index with

the maximum AC power flow to analyze the 118 bus systems. The capacity of the connecting links is defined, and the maximum flow from the source to the sink is calculated. Dey et al [25] investigate the relationship between the topological parameter variation and failure propagation rate in the cascading mechanism through various test beds based on AC power flow equations. Sun et al. [26] propose a cascading failure AC power flow model to discuss the impact of wind power on power systems, and some interesting conclusions are obtained.

AC power flow (ACPF) is employed to analyze power system performance characteristics, where the unbalanced power occurred in the system is completely compensated by a slack node. However, the unbalanced power is usually processed by coordinated dispatching and control of multiple adjustable generating sets in the actual operation. Therefore, a dynamic AC power flow (DACPF) model combined with complex network theory is proposed to discuss power system cascading failure, and then the impact of wind power integration on the power grid is studied more accurately.

This paper is organized as follows. The introduction is displayed in Section 1. Section 2 describes complex network theory in details. Section 3 establishes the DACPF model with complex network theory. Different simulation scenarios are developed in Section 4. Section 5 gives the conclusions.

2. Complex Network Theory

According to graph theory, complex network theory investigates the target system from structure, physical and fault propagation characteristics regardless of the dimensionality of the system overall. It can reveal the operation law of power system, explain the process mechanism of cascading failures, and provide effective measures to reduce and prevent the occurrence of cascading failures or blackouts. The power system can be equivalent to a weighted, directed map on account of complex network theory, where lines are power transmission lines, and nodes are buses.

2.1. Typical Networks

Nowadays, many kinds of complex network models have been proposed, such as the regular network, random network, small-world network, and scale-free network.

Regular network is a symmetric ring, the number of neighboring nodes of each vertex in the network are identical [27]. Then, Erdős and Rényi propose the ER (Erdős and Rényi) random network model [28], where the edge is generated randomly. When the network size is large enough, degree distribution follows the binomial or Poisson distribution, which means the majority of the nodes have similar degree. In addition, Watts and Strogatz construct the WS (Watts and Strogatz) small-world network model, which is between a regular network and random network. Due to a smaller shortest path length as well as a larger clustering coefficient, the speed and the extent of fault propagation of small-world network are higher than those of regular network and random network [29,30]. Studies have shown that the Iranian power grid has obvious small-world property [31], and the medium- and low-voltage power grids of Northern Netherlands are small-world network [32]. Finally, Barabási and Albert establish the BA (Barabási and Albert) scale-free network model [33], which possesses a power-law degree distribution characteristic. It has a handful of core nodes, so that it is vulnerable to deliberate attack but robust against random attacks. The North American power grid has been proved to have prominent scale-free features [34].

2.2. Basic Characteristics

There are four basic characteristics including node degree, clustering coefficient, electrical distance, and electrical betweenness used to interpret complex network theory [26]. Node degree can measure the significance of nodes in the power system. Clustering coefficient describes the tightness and clustering of the whole network. Electrical distance reflects power transmission difficulty and loss in the power grid. Electrical betweenness characterizes the contribution of nodes and edges to power transmission, which is important for the identification of the critical nodes and lines in power system.

3. Complex Network Model

A complex network cascading failure model combined with DACPF is proposed in this section. When failure occurs in the system, current and voltage are used as the boundary conditions to prevent fault propagation. Then, evaluation indicators are adopted to evaluate power grid damage.

3.1. DACPF

There is only a slack node in the calculation of ACPF, that is, all the unbalanced power of the system is compensated by the slack node. For online applications, power imbalance and frequency change in the system are usually caused by line outage, generator failure, load change, and so on. A part of the unbalanced power is adjusted by the load, and most of those are undertaken by the generators. This process is implemented by the coordinated control of multiple generators, not a balancing machine. Therefore, the DACPF is adopted to meet practical needs.

For a given system, the active power flow equation is calculated as follows.

$$P_{Gi} - P_{Di} - P_i(x) = 0, \quad i = 1, 2, \dots, n \quad (1)$$

where P_{Gi} , P_{Di} , $P_i(x)$ are generation, load and power loss of node i , respectively.

If the unbalanced power occurs in power system

$$\Delta P_{\Sigma} = \sum_{i=1}^N P_{Gi} - \sum_{i=1}^N P_{Di} - P_{loss}(x) \quad (2)$$

where P_{loss} is the total transmission loss of power system, which is compensated by all generators.

Then, Equation (1) can be displayed as follows.

$$P_{Gi} - \alpha_i \Delta P_{\Sigma} - P_{Di} - P_i(x) = 0, \quad i = 1, 2, \dots, n \quad (3)$$

where $\alpha_i \left(\sum_{i=1}^n \alpha_i = 1, \alpha_i \geq 0 \right)$ is the proportion of the unbalanced power compensated by generator i .

If the node i is not a generator, or its output power cannot be adjusted, α_i is equal to 0. For the actual system, α_i can be determined by the frequency response coefficient of each generator, certain economic criteria, and so on.

The modification of Jacobian matrix in the ACPF equation is ΔJ due to the introduction of system loss $P_{loss}(x)$. In order to improve calculation efficiency of DACPF, the impact of $P_{loss}(x)$ on the Jacobian matrix is ignored.

In order to correct the active power mismatch in step i of the DACPF iterative calculation, the variation of system loss in step $i - 1$ is given:

$$\Delta P_{loss}(x_{i-1}) = P_{loss}(x_{i-1}) - P_{loss}(x_0) \quad (4)$$

Then, the active equation mismatch of the generator in step i can be obtained.

$$\Delta P'_{Gi} = \Delta P_{Gi} - \alpha_i \Delta P_{loss}(x_{i-1}) \quad (5)$$

Finally, DACPF can be obtained exactly through the above calculations.

3.2. Boundary Conditions

The voltage and current are used as the boundary constraints in the power grid based on DACPF. According to the Motter and Lai model [35], the voltage and current limits of the power network are proportional to their rated voltage and current.

$$U_c = (1 + \beta_U) \cdot U_r \quad (6)$$

$$I_c = (1 + \beta_I) \cdot I_r \quad (7)$$

where U_r, I_r are rated voltage and current; U_c, I_c are the boundaries of voltage and current; β is the tolerance factor, which reveals the ability of the power network to compensate the extra load; $1 + \beta_U$ is the voltage setting coefficient, and $1 + \beta_I$ is the current setting coefficient.

3.3. Evaluation Indicators

Evaluation indicators are used to determine the damaged condition of power system when the network failure occurs.

A. Connectivity

Connectivity is the rate of the node number in maximum power supply radius before and after failure. It reveals the split degree of power system after malfunction.

$$g = \frac{N'}{N} \quad (8)$$

where g expresses connectivity; N and N' indicate the number of nodes in maximum power supply radius before and after failure.

B. Global effective performance

Global effective performance describes the power transmission efficiency.

$$E = \frac{1}{N_G N_L} \sum_{i \in G, j \in L} \frac{1}{d_{ij}} \quad (9)$$

where E expresses global effective performance; subscript G and L represent the sets of generation and load nodes; N_G and N_L display the total number of generation and load nodes; d_{ij} present the shortest electrical distance from generation node i to load node j .

3.4. Simulation Process

- (1) Initial DACPF, including active power, reactive power, voltage and current are calculated based on the given conditions. Then, determine the boundaries of network voltage and current according to Equations (6) and (7).
- (2) Wind power integration.
- (3) Recalculate DACPF of power system, and remove the nodes or edges, whose voltage or current exceed the limit values. Repeat this process until no failure occurs.
- (4) Estimate the impact of wind power on power grid with evaluation index.

4. Case Study

According to topology principles and methods of complex network [26], the IEEE 30 bus system is modeled as a directed, weighted and sparse connected map including 30 nodes and 41 edges, as demonstrated in Figure 1. The advantage of DACPF in cascading failure analysis is discussed in the following applications.

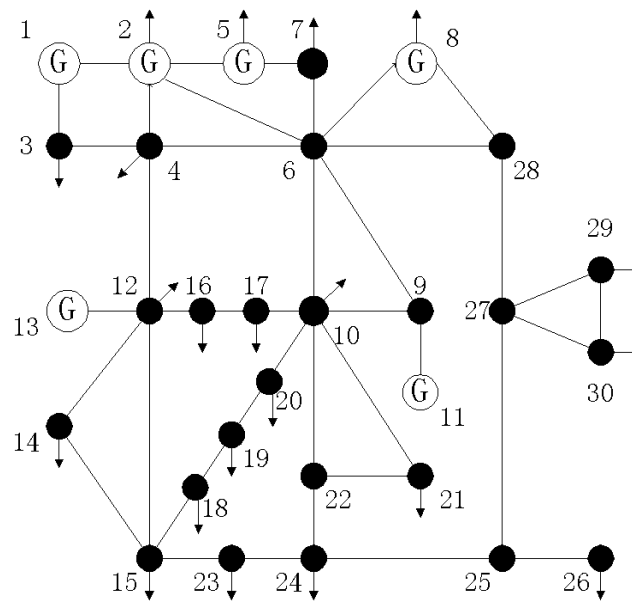
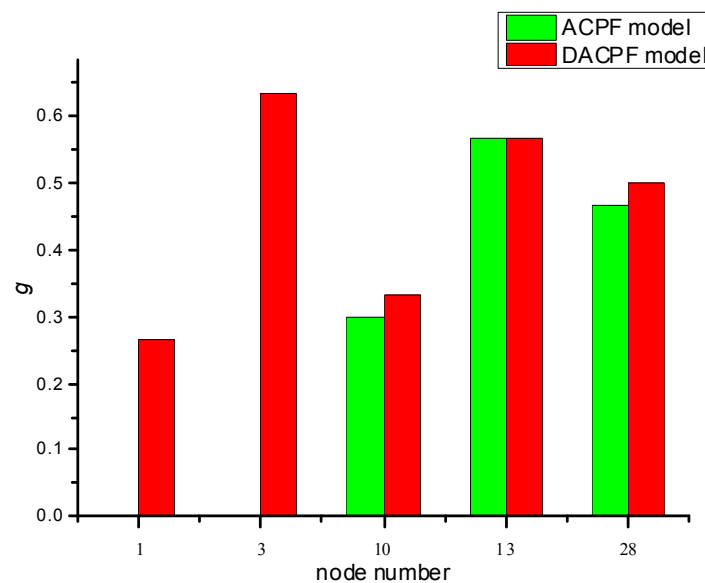


Figure 1. IEEE 30 bus system.

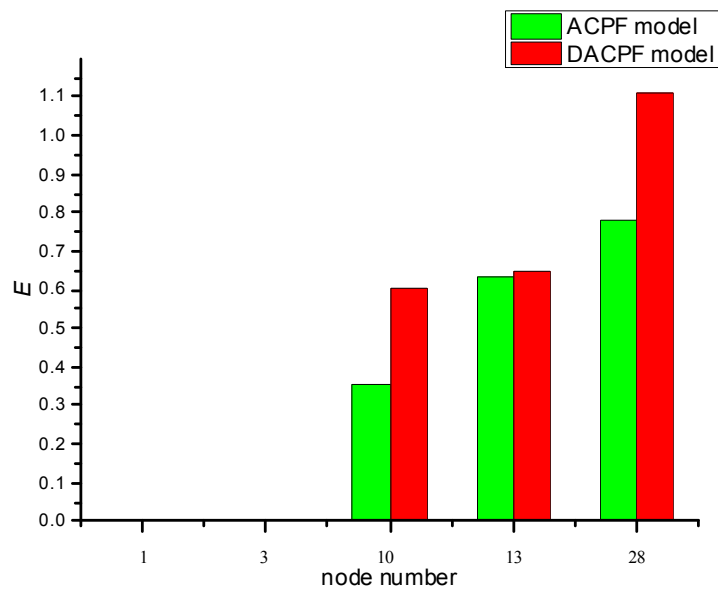
4.1. Impact of Removing Nodes on Power System

The impacts of ACPF and DACPF model on power system are analyzed by nodes removal randomly under the same boundary condition. The simulation results of removing node 1, 3, 10, 13, 28 are shown in Figure 2. Connectivity, that is, g , of ACPF and DACPF model are identical when node 13 is removed, while the former is less than the latter by removing other nodes. Global effective performance, that is, E , of ACPF and DACPF model are both 0 by removing node 1 and node 3. However, global effective performance of DACPF model is larger than that of ACPF model when other nodes are removed. Therefore, it is more reasonable for DACPF model to analyze power system cascading failure triggered by nodes removal.



(a)

Figure 2. Cont.



(b)

Figure 2. Contrastive analysis of the impacts of removing nodes, (a) Connectivity; (b) Global effective performance.

4.2. Impact of Wind Power Integration on Power System

From Figure 3, the installed capacity of the wind farm is 100 MW and the sampling interval is minute level. Its output power varies greatly. In order to improve the ability of power systems to accept wind power, wind farm power output fluctuation is mitigated by the energy storage system with a flexible first-order low-pass filter control strategy [36]. Wind power after smoothing is flat, which is shown in Figure 4.

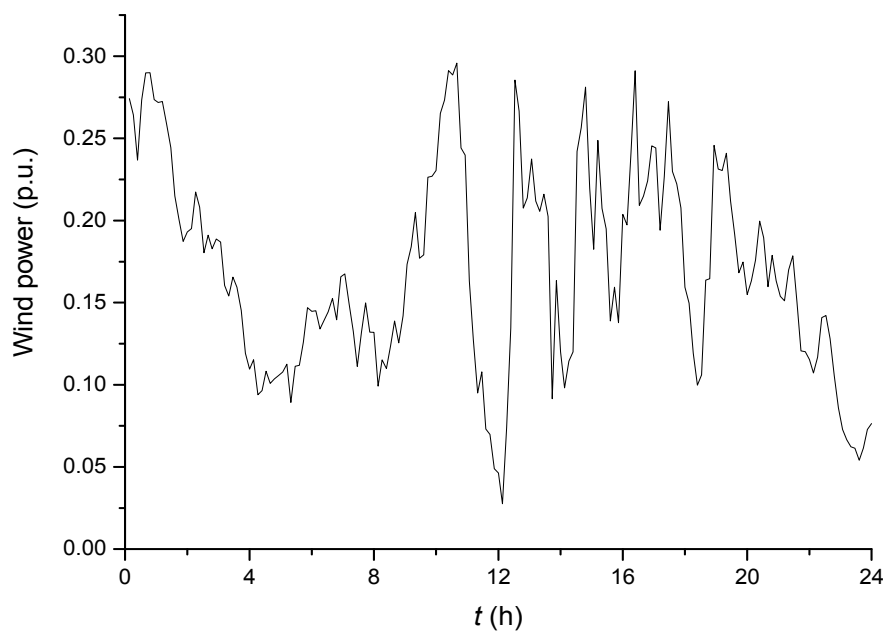


Figure 3. Wind power over the course of a day.

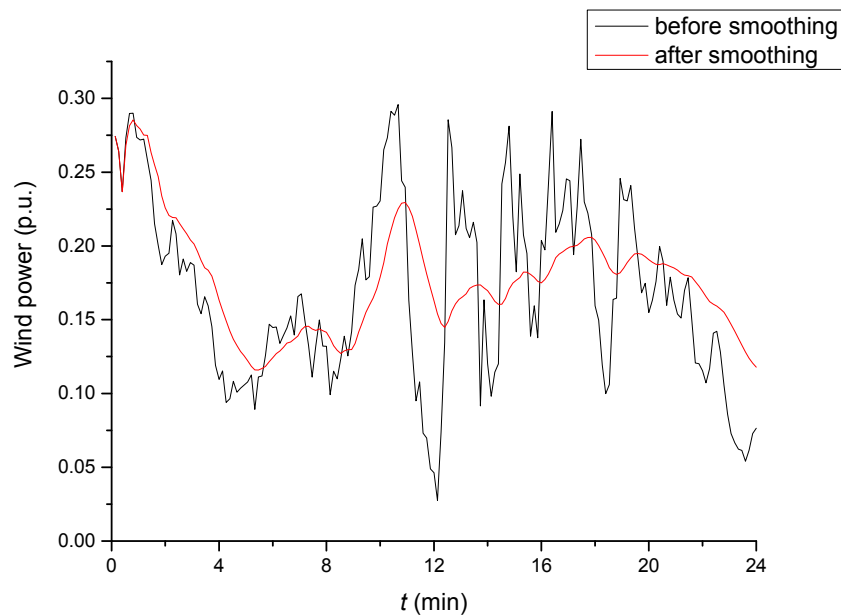


Figure 4. Wind power before and after smoothing.

In addition, Figure 5 indicates that the max 30-min wind power fluctuation rate before smoothing is 25.79%, while the one after smoothing is less than 7%. Therefore, wind power has been smoothed effectively. Wind power fluctuation rate is calculated as follows.

$$f = \frac{\max(P_{1,2\dots k}) - \min(P_{1,2\dots k})}{P_{rated}} \quad (10)$$

where $P_{1,2\dots k}$ is wind power at time k ; P_{rated} is the installed capacity of wind power.

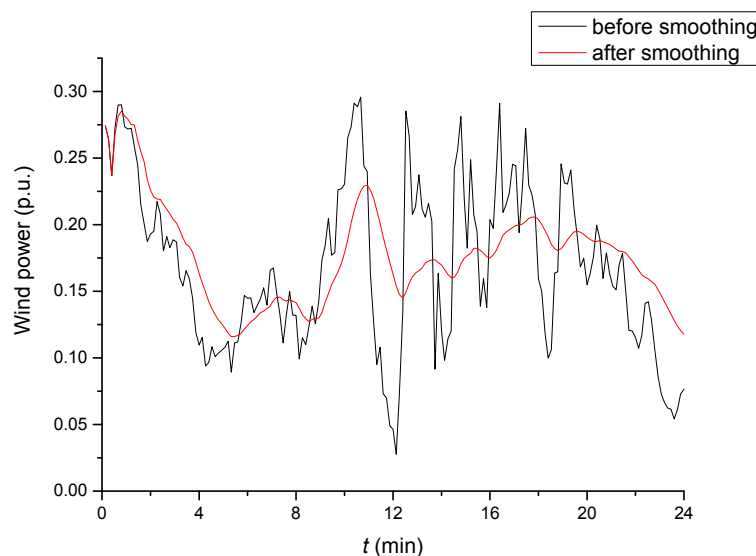


Figure 5. Wind power fluctuations before and after smoothing.

In the following analysis, wind power is used to represent the generator node 13 in the IEEE 30 bus system. Then, the rationality and validity of DACPF model are analyzed compared with ACPF model from section A to C. In addition, some significant analysis is implemented based on DACPF model in section D and E.

A. Contrastive analysis of the impact of wind power

The power grid can accept more wind power after smoothing with smaller power fluctuation. Therefore, the generator node 13 is replaced by wind power after smoothing with the same installed capacity. As can be obtained from Figure 6, the connectivity and global effective performance of the DACPF and ACPF models vary with the change of wind power. Additionally, the former connectivity and global effective performance are larger than the latter ones, that is, the influence of wind power on power grid can be better reflected by the DACPF model.

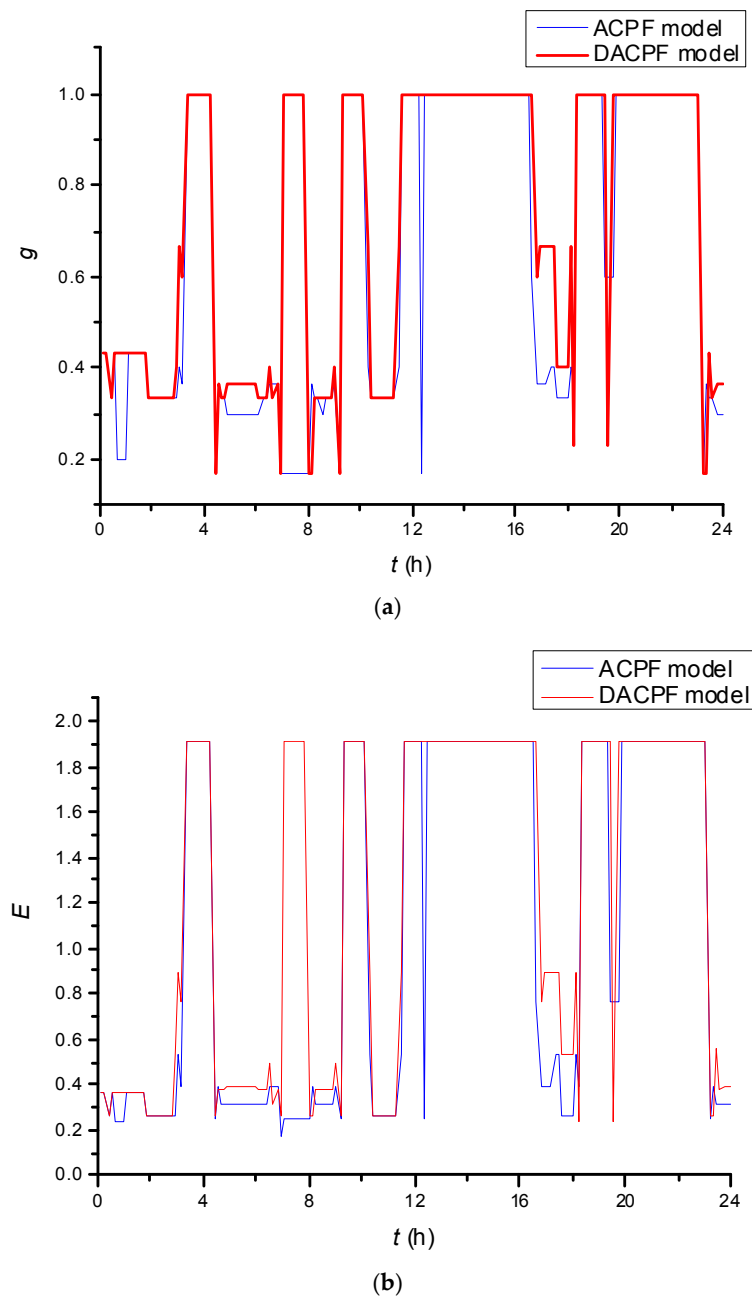


Figure 6. Comparative analysis of the impacts of wind power, (a) Connectivity; (b) Global effective performance.

B. Contrastive analysis of the impact of grid current tolerance capability

The impact of wind power (after smoothing) on power system is displayed in Figure 7, which is obtained by adjusting the current setting coefficient with a fixed voltage limit. Connectivity and global effective performance of DACPF model are larger than those of ACPF model when the current setting coefficient is less than 1.4. If the current setting coefficient is over 1.4, they are the same. Hence, it is more meaningful for DACPF model to discuss the impact of wind power on a power grid within the effective current boundary condition.

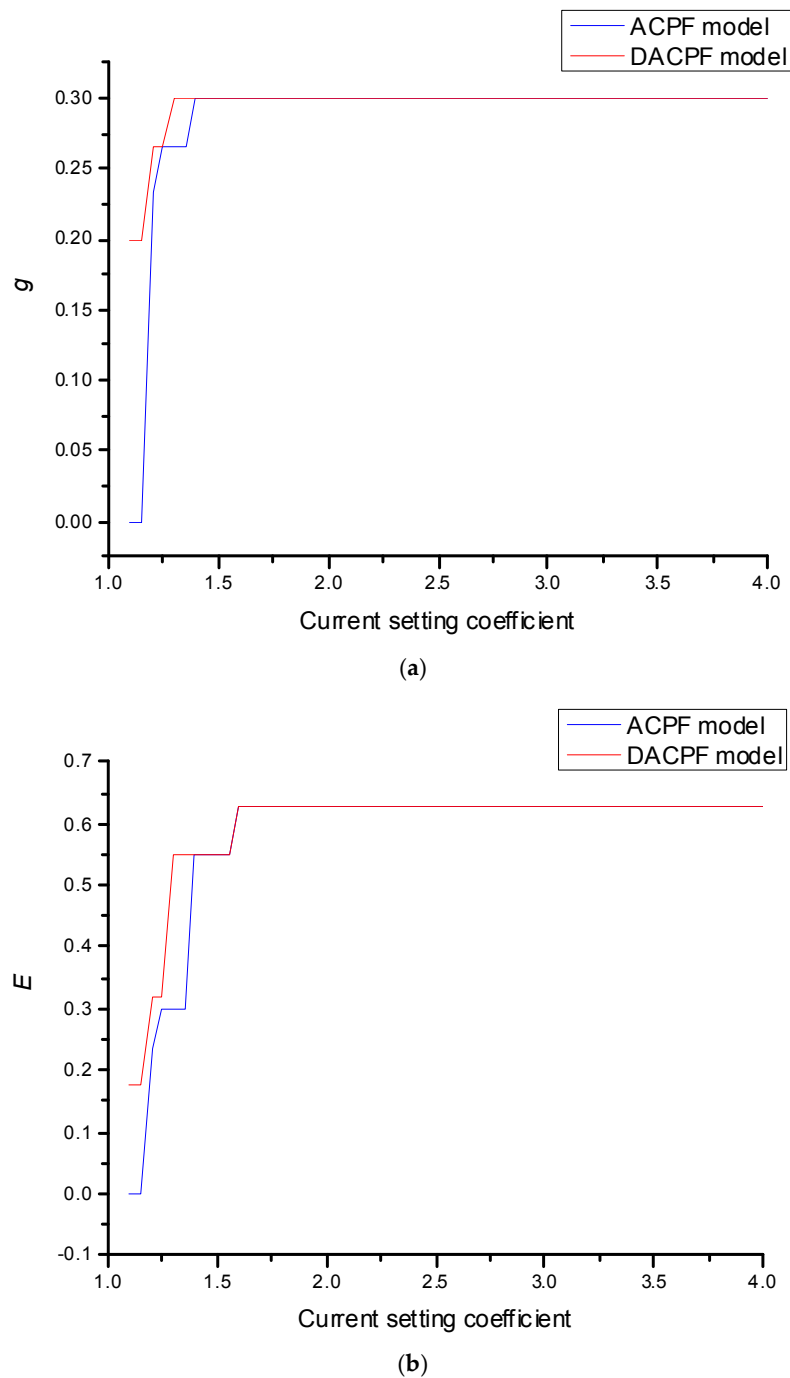


Figure 7. Comparative analysis of the impact of grid current tolerance capability, (a) Connectivity; (b) Global effective performance.

C. Contrastive analysis of the impact of grid voltage tolerance capability

The influence of wind power (after smoothing) on power grid is studied by adjusting the voltage setting coefficient at a fixed current limit. As can be seen from Figure 8, connectivity of DACPF and ACPF model are identical when the voltage setting coefficient is less than 1.056. The former is superior to the latter if the voltage setting coefficient is over 1.056. Furthermore, global effective performance of the DACPF model has a larger value with the change of the voltage setting coefficient. Therefore, the DACPF model has good simulation results within the effective voltage boundary condition.

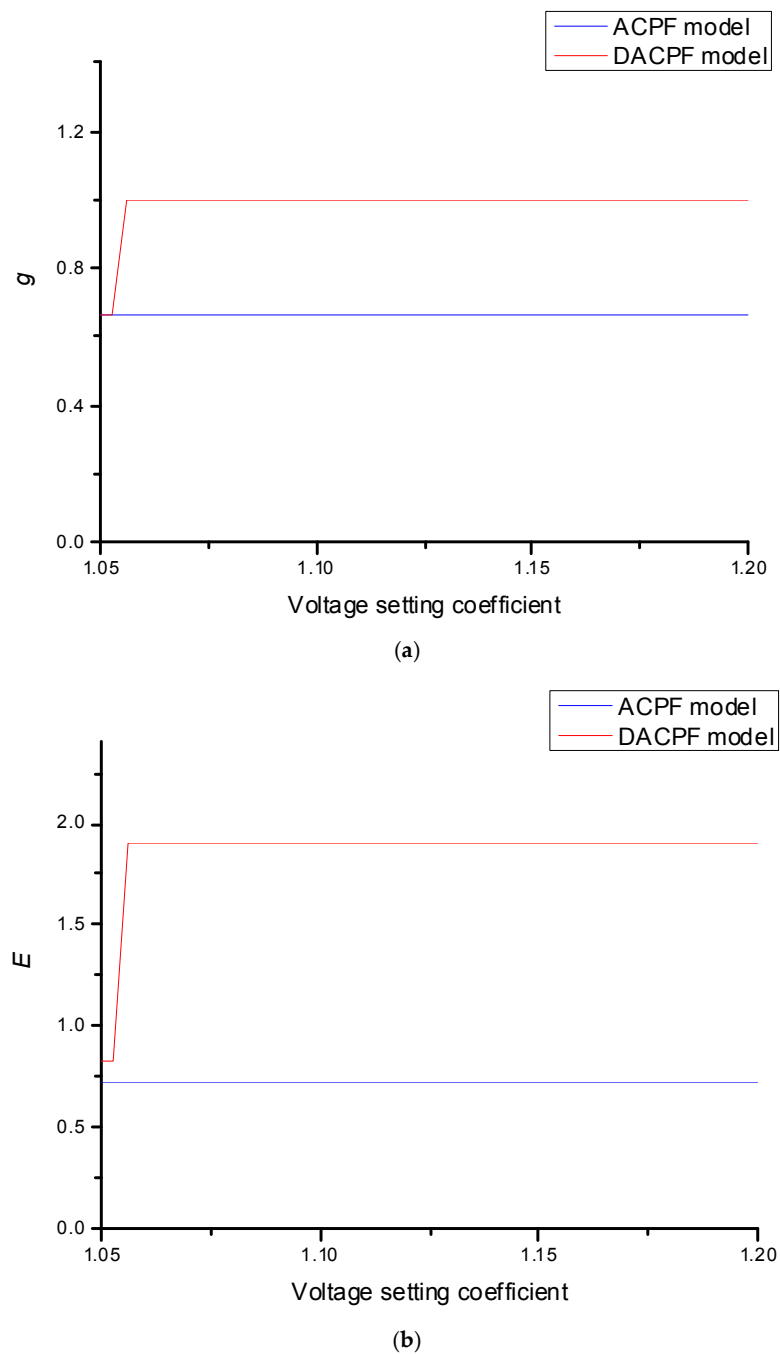


Figure 8. Comparative analysis of the impact of grid voltage tolerance capability, (a) Connectivity; (b) Global effective performance.

D. Contrastive analysis of the impact of wind power before and after smoothing

Based on the DACPF model, the generator node 13 is represented by wind power before and after smoothing in Figure 4, respectively. The connectivity and global effective performance of wind power after smoothing are greater than the ones before smoothing. In other words, wind power after smoothing has less effect on power system, which can be obtained from Figure 9. So it is necessary to smooth the wind power fluctuation from the view of complex network theory.

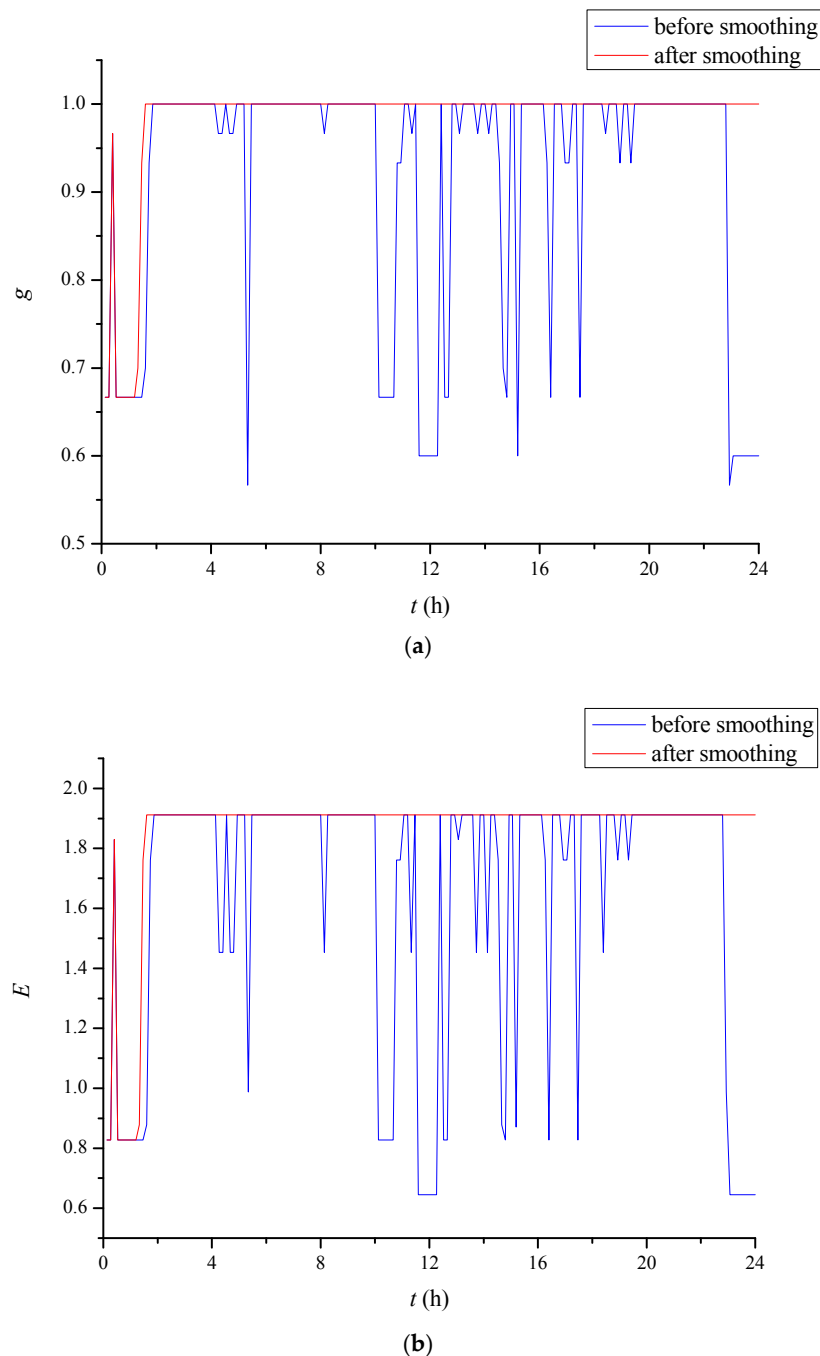


Figure 9. Comparative analysis of the impacts of wind power before and after smoothing, (a) Connectivity; (b) Global effective performance.

E. Contrastive analysis of the impacts of different wind power coupling locations

Based on the DACPF model, the impact of different wind power (after smoothing) coupling locations is analyzed. From Figure 10, node 6 with larger degree and electric betweenness, and node 29 with smaller those are selected as the points of wind power integration, respectively. The connectivity of node 6 is larger than that of node 29 from 0 h to 2.4 h and from 10.4 h to 11.2 h. Moreover, the global effective performance of node 6 is always higher than that of node 29 in a day. In a word, the selection of greater degree and electric betweenness node for wind power coupling point has less impact on power grid performance.

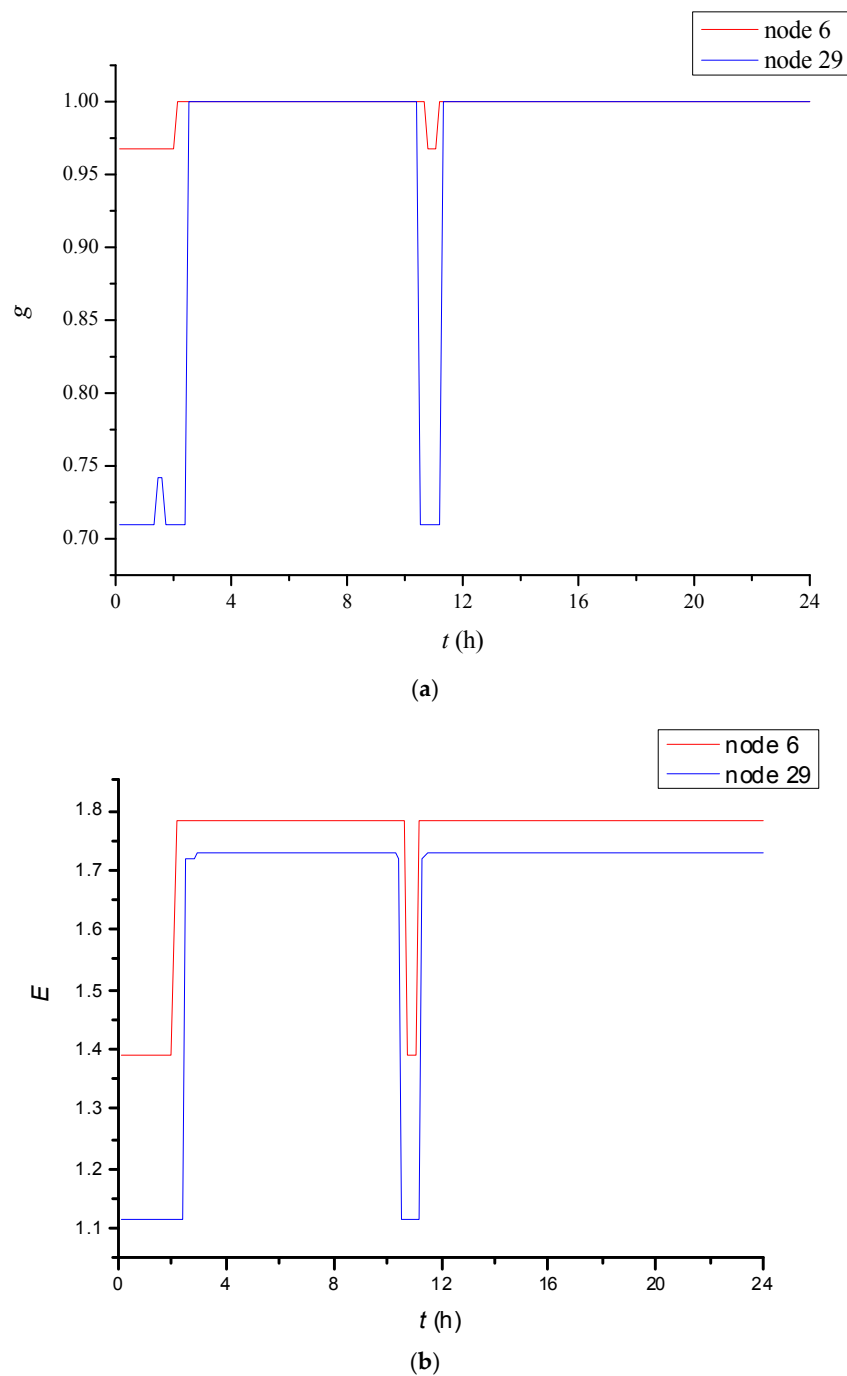


Figure 10. Comparative analysis of the impacts of different wind power coupling locations, (a) Connectivity; (b) Global effective performance.

5. Conclusions

The impact of wind power on power grid is discussed with complex network theory in this paper. Firstly, a DACPF cascading failure model is established on the basis of the IEEE 30 bus system. Then, comparative analysis of the ACPF and DACPF models is implemented by nodes removal, wind power integration and the change of current and voltage boundaries. The validity of the DACPF model based complex network theory is verified. In addition, wind power after smoothing has less impact on power system compared with wind power before smoothing. The reason why grid-connected wind power should be mitigated is interpreted based on complex network theory. Finally, selecting larger degree and electric betweenness node as wind power coupling point can reduce the impact on power systems.

Acknowledgments: This work was financially supported by a grant from the National Key Research and Development Program of China (No. 2016YFB0900400) and Foundation of Director of Institute of Electrical Engineering, Chinese Academy of Sciences (No. Y760141CSA) and Jiangsu Province 2016 Innovation Ability Construction Special Funds (No. BM2016027).

Author Contributions: Yushu Sun and Xisheng Tang conceived and designed the simulation and experiment. Guowei Zhang provided the simulation and experimental platform. Fufeng Miao worked on the simulation and the writing of paper. Ping Wang analyzed the data.

Conflicts of Interest: The authors declare no conflict of interest.

References

1. US-Canada Power System Outage Task Force. *Final Report of the August 14th Blackout in US and Canada*; United States Department of Energy and National Resources Canada: Washington, DC, USA; Ottawa, ON, Canada, 2004.
2. National Grid Company. *Investigation Report into the Loss of Supply Incident Affecting Parts of South London at 18:20 on Thursday*; Technical Report; National Grid UK: London, UK, 2003.
3. Chowdhury, T.; Chakrabarti, A.; Chanda, C.K. Analysis of vulnerability indices of power grid integrated DG units based on complex network theory. In Proceedings of the IEEE India Conference, New Delhi, India, 17–20 December 2015.
4. Wang, Z.Y.; Chen, G.; Hill, D.J.; Dong, Z.Y. A power flow based model for the analysis of vulnerability in power networks. *Physica A* **2017**, *460*, 105–115. [[CrossRef](#)]
5. Luo, G.; Shi, D.G.; Chen, J.F.; Duan, X.Z. Automatic identification of transmission sections based on complex network theory. *IET Gener. Transm. Distrib.* **2014**, *8*, 1203–1210.
6. Chu, C.C.; Iu, H.H.C. Complex networks theory for modern smart grid applications: A survey. *IEEE J. Emerg. Sel. Top. Circuits Syst.* **2017**, *7*, 177–191.
7. Correa, G.J.; Yusta, J.M. Grid vulnerability analysis based on scale-free graphs versus power flow models. *Electr. Power Syst. Res.* **2013**, *101*, 71–79.
8. Fan, W.L.; Liu, Z.G.; Hu, P.; Mei, S.W. Cascading failure model in power grids using the complex network theory. *IET Gener. Transm. Distrib.* **2016**, *10*, 3940–3949.
9. Yin, R.R.; Liu, B.; Liu, H.R.; Li, Y.Q. Research on invulnerability of the random scale-free network against cascading failure. *Physica A* **2016**, *444*, 458–465.
10. Zhang, W.; Pei, W.; Guo, T.D. An efficient method of robustness analysis for power grid under cascading failure. *Saf. Sci.* **2014**, *64*, 121–126.
11. Liu, J.; Xiong, Q.Y.; Shi, X.; Wang, K.; Shi, W. Robustness of complex networks with an improved breakdown probability against cascading failures. *Physica A* **2016**, *456*, 302–309.
12. Zhang, J.H.; Xu, X.M.; Hong, L.; Wang, S.L.; Fei, Q. Attack vulnerability of self-organizing networks. *Saf. Sci.* **2012**, *50*, 443–447.
13. Wang, J.W.; Rong, L.L. Robustness of the western United States power grid under edge attack strategies due to cascading failures. *Saf. Sci.* **2011**, *49*, 807–812.
14. Wang, J.W.; Rong, L.L. Vulnerability of effective attack on edges in scale-free networks due to cascading failures. *Int. J. Mod. Phys. C* **2009**, *20*, 1291–1298. [[CrossRef](#)]

15. Peng, X.Z.; Yao, H.; Du, J.; Wang, Z.; Ding, C. Invulnerability of scale-free network against critical node failures based on a renewed cascading failure model. *Physica A* **2015**, *421*, 69–77. [[CrossRef](#)]
16. Nicholson, C.D.; Barker, K.; Ramirez-Marquez, J.E. Flow-based vulnerability measures for network component importance: Experimentation with preparedness planning. *Reliab. Eng. Syst. Saf.* **2016**, *145*, 62–73. [[CrossRef](#)]
17. Bompard, E.; Pons, E.; Wu, D. Extended topological metrics for the analysis of power grid vulnerability. *IEEE Syst. J.* **2012**, *6*, 481–487. [[CrossRef](#)]
18. Bompard, E.; Wu, D.; Xue, F. Structural vulnerability of power systems: A topological approach. *Electr. Power Syst. Res.* **2011**, *81*, 1334–1340. [[CrossRef](#)]
19. Yan, J.; He, H.B.; Sun, Y. Integrated security analysis on cascading failure in complex networks. *IEEE Trans. Inf. Forensics Secur.* **2014**, *9*, 451–463. [[CrossRef](#)]
20. Lin, Z.Z.; Wen, F.S.; Xue, Y.S. A restorative self-healing algorithm for transmission systems based on complex network theory. *IEEE Trans. Smart Grid* **2016**, *7*, 2154–2162. [[CrossRef](#)]
21. Yan, J.; Tang, Y.F.; He, H.B.; Sun, Y. Cascading failure analysis with DC power flow model and transient stability analysis. *IEEE Trans. Power Syst.* **2015**, *30*, 285–297. [[CrossRef](#)]
22. Qi, H.B.; Shi, L.B.; Ni, Y.X.; Yao, L.Z.; Masoud, B. Study on power system vulnerability assessment based on cascading failure model. In Proceedings of the 2014 IEEE PES General Meeting Conference & Exposition, National Harbor, MD, USA, 27–31 July 2014; pp. 1–7.
23. Chen, G.; Dong, Z.Y.; Hill, D.J.; Zhang, G.H.; Hua, K.Q. Attack structural vulnerability of power grids: A hybrid approach based on complex networks. *Physica A* **2010**, *389*, 595–603. [[CrossRef](#)]
24. Dwivedi, A.; Yu, X.H. A maximum-flow-based complex network approach for power system vulnerability analysis. *IEEE Trans. Ind. Inform.* **2013**, *9*, 81–88. [[CrossRef](#)]
25. Dey, P.; Mehra, R.; Kazi, F.; Wagh, S.; Singh, N.M. Impact of topology on the propagation of cascading failure in power grid. *IEEE Trans. Smart Grid* **2016**, *7*, 1970–1978. [[CrossRef](#)]
26. Sun, Y.S.; Tang, X.S. Cascading failure analysis of power flow on wind power based on complex network theory. *J. Mod. Power Syst. Clean Energy* **2014**, *2*, 411–421. [[CrossRef](#)]
27. Sole, R.V.; Valverde, S. Information transfer and phase transitions in a model of internet traffic. *Physica A* **2001**, *289*, 595–605. [[CrossRef](#)]
28. Erdős, P.; Rényi, A. On the evolution of random graphs. *Publ. Math. Inst. Hung. Acad. Sci.* **1960**, *5*, 17–61.
29. Watts, D.J.; Strogatz, S.H. Collective dynamics of “small—World” networks. *Nature* **1998**, *393*, 440–442. [[CrossRef](#)] [[PubMed](#)]
30. Newman, M.E.J.; Watts, D.J. Renormalization group analysis of the small-world network model. *Phys. Lett. A* **1999**, *263*, 341–346. [[CrossRef](#)]
31. Monfared, M.A.S.; Jalili, M.; Alipour, Z. Topology and vulnerability of the Iranian power grid. *Physica A* **2014**, *406*, 24–33. [[CrossRef](#)]
32. Pagani, G.A.; Aiello, M. Towards decentralization: A topological investigation of the medium and low voltage grids. *IEEE Trans. Smart Grid* **2011**, *2*, 538–547. [[CrossRef](#)]
33. Barabási, A.L.; Albert, R. Emergence of scaling in random networks. *Science* **1999**, *286*, 509–512. [[PubMed](#)]
34. Albert, R.; Albert, I.; Nakarado, G.L. Structural vulnerability of the North American power grid. *Phys. Rev. E* **2004**, *69*, 025103(R). [[CrossRef](#)] [[PubMed](#)]
35. Lai, Y.C.; Motter, A.E.; Nislikawa, T. Attacks and cascades in complex networks. *Lect. Notes Phys.* **2004**, *650*, 299–310.
36. Jiang, Q.Y.; Gong, Y.Z.; Wang, H.J. A battery energy storage system dual-layer control strategy for mitigating wind farm fluctuations. *IEEE Trans. Power Syst.* **2013**, *28*, 3263–3273. [[CrossRef](#)]

